Turkish Journal of Computer and Mathematics Education Vol.12 No. 11 (2021), 2522- 2538
Research Article

Autopilot construction in the longitudinal and transverse sections of a plane using adaptive

Khwther Abbodd Neamah[*1], Safa Abood Nama[2]

Iraq/Baghdad College of Economics Sciences University[1]
Iraq/ALiraqia University, college of engineering[2]
cs@baghdadcollege.edu.iq

Article History: Received: 11 January 2021; Revised: 12 February 2021; Accepted: 27 March 2021; Published online: 10 May 2021

Abstract
In this research, a simulation model of a non-linear model for unmanned neural vehicles is developed using Airsim (simulator via an open-source platform for drones and ground vehicles). The non-linear model of the vehicle is approximated as a linear model with a balance point in the first stage. With this model, a conventional controller is designed to have longitudinal and transverse sections, and this controller is added to the non-linear model. Then, a neural network is introduced to the traditional controller to perform the error compensation process after the approximation of the non-linear model with a linear model. The calculated results from the neural network that depended upon the error process are added to the results that obtained from the non-Linear model and the linear model to the conventional microcontroller. Results show that the adaptive controller could achieve stability for the system for a wide range of aviation envelope. Thus, the use of an adaptive controller that consists of a traditional controller and a neurological compensator can compensate for various disorders that may occur in vehicles, such as changes in altitude, direction and pressure disturbance .

Keywords: Adaptive control, drone, neuronal compensator, directional rudder, deeper rudder

Introduction

1.Many studies focused on the external stimuli that the plane is subject to during flight. For instance, [2] focused in determining the main equations required to build a simulation environment for the plane that is as near as possible to reality. In [4], authors suggested an approach to designing an adaptive controller for a drone that relies on neural networks with an algorithm that works in real time. The network weights are adjusted according to the system's state transformation errors by minimising a specified cost function according to Lyapunov's second theory. Consequently, the need for advance data for training the network was eliminated. Here, the control signal that the neural network provides is combined with the external control signal from a traditional controller to compensate- for the disturbances plane Model 15 are subject to.

In [5], a new way of designing a four-fan adaptive console that relies on neural networks is proposed. The main idea is to use two neural networks on branching instead of one in the closed-loop to determine the non-linear changes in the dynamism of the hovercraft (which is a vehicle floating in air with an airbag below its body).

The weights of the two networks are modified using a tab function using Lyapunov theory. [7] combined a floating system and a neural network to design a hybrid system for controlling a drone in an environment that is not clear-cut[1-5] .

Traditional and hybrid controls are adopted to show the advantages of using the proposed controller. Comparison indicates that unlike the traditional controller, the hybrid controller could adapt to the turbulence and change the mechanism of work.

In this research, we built a pilot. Adaptive neural control is used in the longitudinal and transverse sections of the plane. The controller must be able to stabilise the plane in the longitudinal and transverse sections with the height change within a specific area of envelope aviation [6-10].

We rely on this research on the accumulated information about control theories on and on some references and websites. Several tools were used for research, such as Matlab for simulating the theories. Then, the same special programs were used to model the physical components of the plane, and from Design and Selection of Controllers using the Simulink to L in Matlab.

1.1 Mechanism of the drone work

This aircraft is categorised as a small drone and mainly designed to act as a surveillance device in remote weather conditions and dangerous areas. In terms of control, the plane is fully automatic and

easy to program to complete the required tasks. The aircraft weighs approximately 14–15 kg and can fly to an altitude range of 700–750 m and carry loads in the weight range of 2–6 kg, corresponding to a flight time of 10.30 h.[22-26]
Figure (1) shows that the fuselage represents the deflection angles and the steering rudders control the relay and front wing Ailerons to centre the coup.

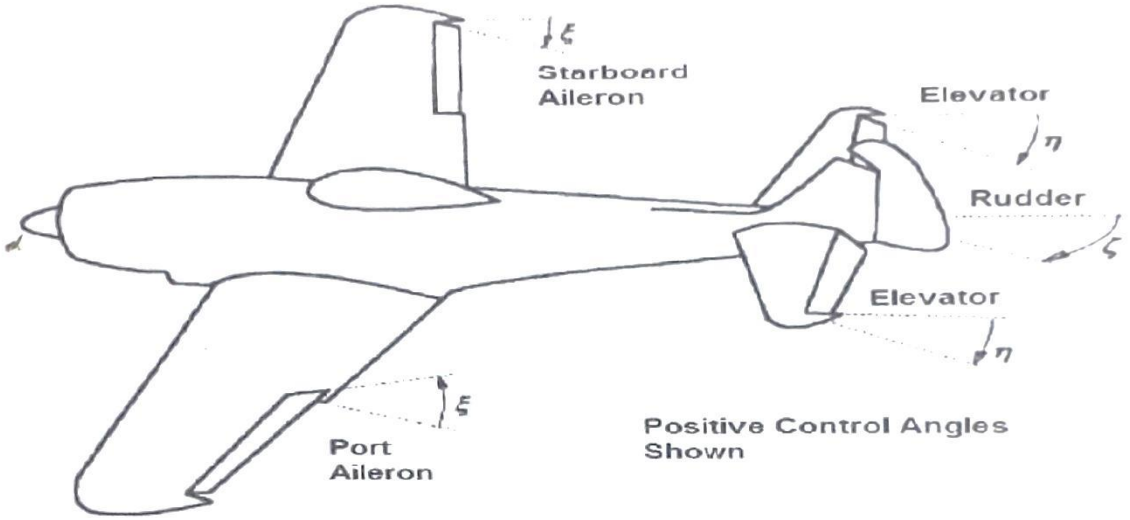

1.2 Motion equations
In [9], mathematical equations for the plane motion in air are presented. $(x\ y\ z\ ) + mg_o(-sin\ (\theta)\ cos\ cos\ (\theta)\ sin\ (\emptyset)\ \ cos\ cos\ (\theta)\ cos\ (\emptyset)\ ) = M\big(\dot{u} + qw - ru\ \dot{V} + ru - pw\ \dot{W} + pv - qu\ \big)$

$$L = I_x\dot{p} + \big(I_z - I_y\big)qr$$

$$M = I_y\dot{q} + (I_x - I_z)pr$$

$$N = I_z\dot{r} + \big(I_y - I_x\big)qp$$

The equations above reveal that the variables of the plane's body condition in terms of angles, speed, forces and torque are as follows:
1) The angle represents height $\emptyset$, the angle of delinquency $\emptyset$, the angle of direction Ψ, the angle of attack x, slide angle β and track angle Y.

2. Forward linear velocity u, lateral linear velocity V, vertical linear Velocity w, the p angular velocity around axis x, the qangular velocity around axis y and the rangular velocity around axis z [26-29].
3. The thrust force in forwarding direction x, the thrust force in the lateral direction, the thrust force in vertical direction z, the L torque around axis x, the M torque around axis y and the N torque around axis z.
We study the aircraft system with specific work points for the design of the conventional controller. Therefore, we must approximate non-linear equations with these work points and have a process of approximating linear mathematical equations for the plane's movement which has a specific work point. We divide the equations into two parts. The first part concerns the movement of the longitudinal section, and the other part concerns the movement of the plane in the cross-section.

1.3 Motion equations with two syllables (longitudinal and transverse)
We form the following motion equations with two syllables, i.e. longitudinal and transverse:

$$\begin{bmatrix} \dot{u} \\ \dot{w} \\ \dot{q} \\ \dot{\theta} \end{bmatrix} = \begin{bmatrix} \frac{X_u}{m} & \frac{X_w}{m} & -W_o & -g \\ \frac{Z_u}{m} & \frac{Z_w}{m} & U_o & o \\ o & \frac{M_w}{I_y} & \frac{M_q}{I_y} & o \\ o & o & I & o \end{bmatrix} \begin{bmatrix} u \\ w \\ q \\ o \end{bmatrix} + \begin{bmatrix} o \\ \frac{Z_n}{m} \\ \frac{M_n}{I_y} \\ o \end{bmatrix} [\eta]$$

$$\begin{bmatrix} \dot{v} \\ \dot{p} \\ \dot{r} \\ \dot{\phi} \end{bmatrix} = \begin{bmatrix} \frac{Y_v}{m} & W_o & -U_o & g \\ \frac{L_y}{I} & \frac{L_p}{I_x} & \frac{L_y}{I_x} & o \\ \frac{N_v}{I_z} & \frac{N_p}{I_z} & \frac{N_r}{I_z} & o \\ o & I & o & o \end{bmatrix} \begin{bmatrix} v \\ p \\ r \\ \phi \end{bmatrix} + \begin{bmatrix} \frac{Y}{m} & o \\ \frac{L_S}{I} & \frac{L_S}{I_x} \\ \frac{N_S}{I_z} & \frac{N_S}{I_z} \\ o & o \end{bmatrix} [S\ S\ ]$$

where $X_u, X_w, Y_v, Z_w, L_p, M_g, I_r, \dots, etc.$ are the derivatives of forces and moments attributed to a change in one of the variables. It is a fixed ground gravity (g), and it is the mass of the plane m. U_o and W_o are the plane's front and vertical speeds, respectively, at the work points concerning the cross-section. The plane moves in the cross-section due to the change in the angles of the directional flank and the Pavilion, thereby changing the velocities of the lateral plane and the three angle changes. Linear motion equations are also formed in the cross-section, where $I_x, Y_v, N_r, N_p, L_s, N_v, I_z, \dots, etc.$ are the derivatives of forces and moments in relation to a change in a variable. g is the fixed ground gravity, m is the mass of the plane, and U_o and W_o are the plane's front and vertical speeds at the work points.

2. Design of traditional laws of control

The traditional control laws of conventional PID controls are designed in both longitudinal and transverse sections. Initially, the parameter values were determined for matrices A, ctrl B and observe c (where D = o casual system). The Aerorasim software which has a work point (altitude 250 m, speed 35 m/s) was also used. Figure(2) shows a box diagram for simulating the conventional controller in the longitudinal section.

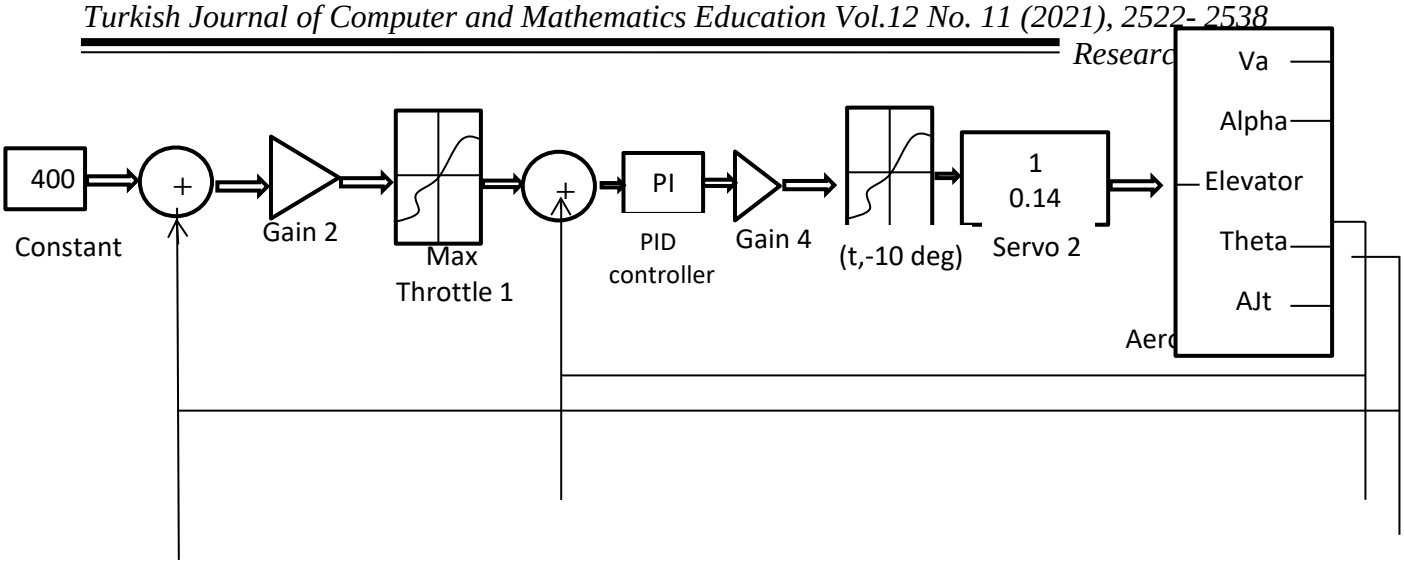

Figure (2) is a box diagram drawing of a simulation of the diving altitude controller and the traditional elevation angle

In the longitudinal section, the diving angle parameters Kd = 1 - 5, ki = 2.5, and kp = 8.5 were set to obtain a response time of 1 s. After less than 25% passes after the successful installation of the conventional diving angle controller, the elevation ring was closed so that the outer ring was the angle of the diving ring. We only needed a relative controller here. Kp = 3 to control the height of the plane after adjusting the angle of diving. Then, a PID type controller was installed to control the speed ring (i.e. kd = 3, ki = 0.5 and kp = 1.8) so that the plane achieved the maximum possible speed within 2 s.
Relative to the cross-section, the conventional (PI) controller is designed to control the closed loop at the angle of misdemeanour so that KP = 0.8, ki = 0.05 and the proportional control unit design is only pk = 0.1 to control the closed circuit at an angle of direction.

2.1 The results of traditional controller application in the cross and longitudinal section

Figure (3) shows the response of the closed loop at the height (one hopl) of 300 m, where the plane should travel from the height of loom to 400 m.
Figure (4) shows the closed-loop response to the diving angle during this transition, while Figure (5) shows the closed-loop response at the plane speed of 30 m/s during this transition.
Figure (6) shows the response of the closed-loop at an angle of direction of 20°. In contrast, Figure (7) illustrates the behaviour of the closed-loop at the angle of delinquency during the change in direction angle.

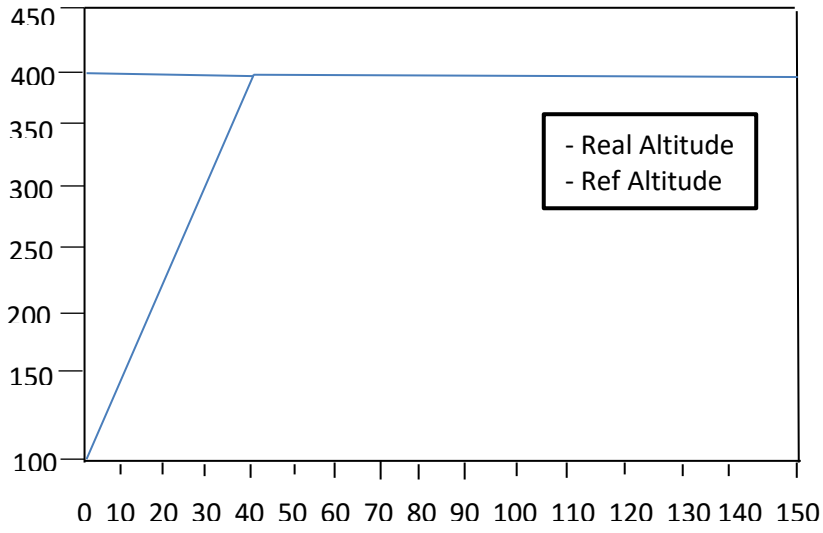

Figure (3): The closed loop response

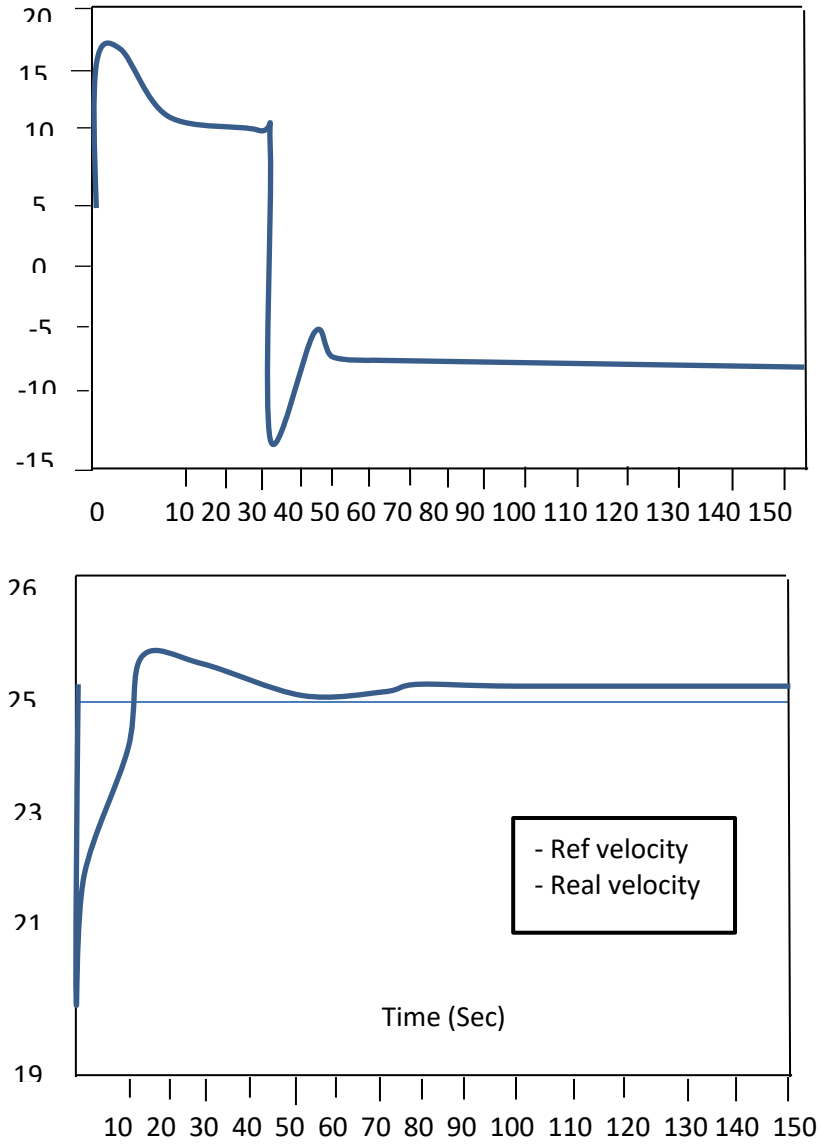

Figure (5): The closed loop response quickly as the height changes

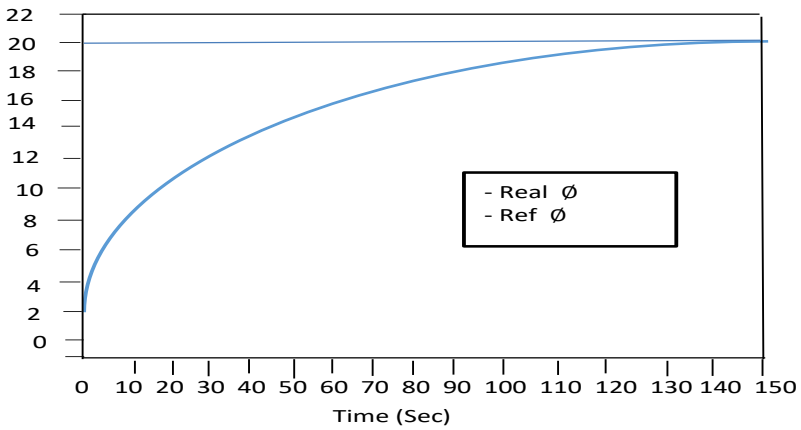

Figure (6): The closed loop response an angle of direction

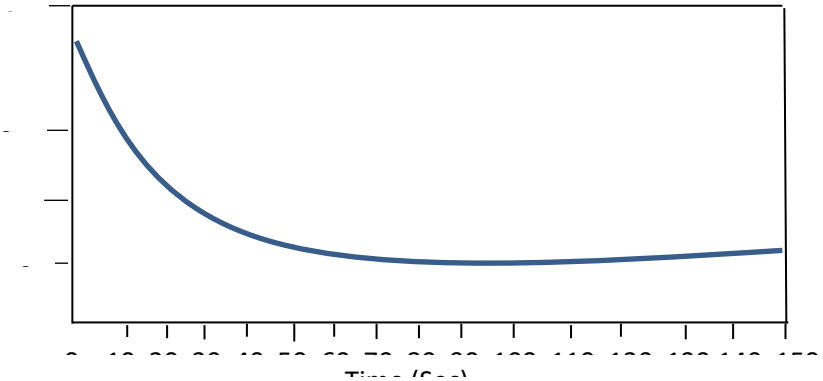

Figure (7) changes in the angle of delinquency during the change in the angle of direction

2.2 Test the perform

In this stage, the performance of the conventional controllers in the longitudinal and transverse sections is tested to measure the largest field in which the plane remains stable with the presence of these controls without the need for adaptation. Result shows that the traditional cross-section controller remained able to stabilise the plane up to a height of 2000 m, while the traditional controller in the longitudinal section lost its ability to control the plane when the height changes from the rank of 300 m. These issues are due to the large change in plane parameters in the longitudinal section with the changes in behaviour, such as pressure and the gravitational force of the Earth.

To perform this test, the different status, control and monitoring matrices are calculated with several work points within the field [2000–300]. The application of traditional controls is divided into two systems in the longitudinal and transverse sections. Figure (8) shows the response of the closed ring with the diving angle for the work point corresponding to the height of 1000 m. Meanwhile, Figure (9) shows the response of the closed-loop system in the direction angle at this point of action.

Pitch –to-elevator (PID) controller

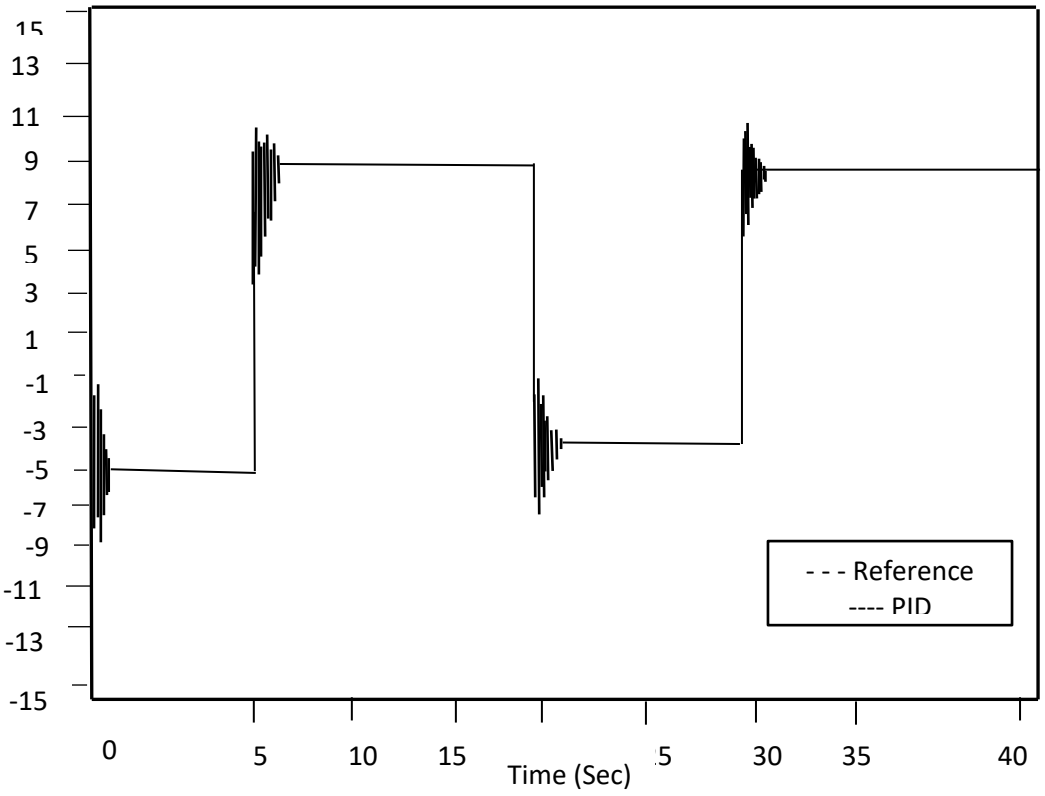

Figure (8): The closed-loop system in the diving angle of responded with the change of the work point

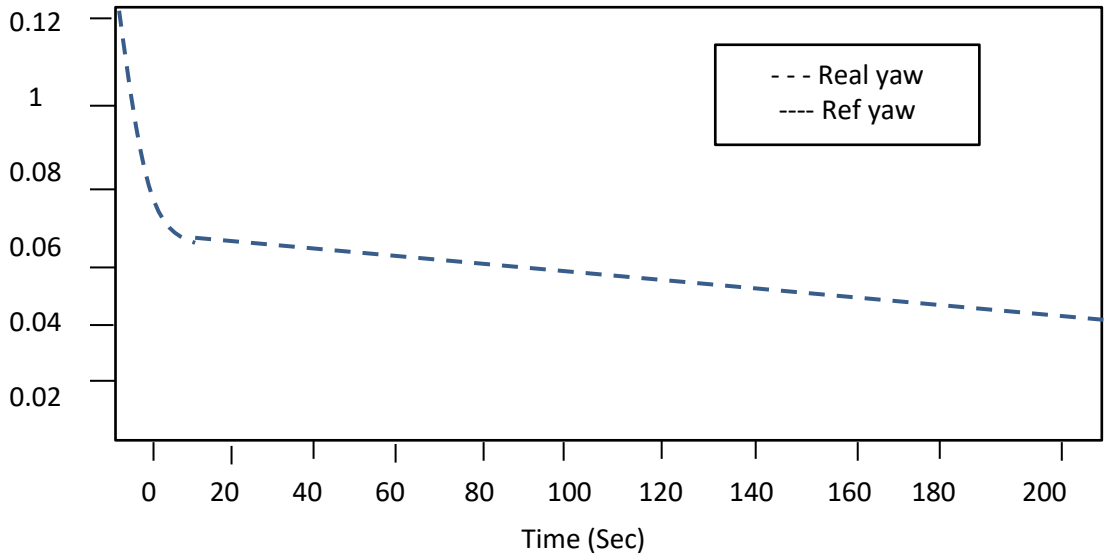

Figure (9): The closed-loop response system at an angle of direction with the change of the action point

Figure (8) clearly shows that the closed-loop system in the longitudinal section can generally stabilise the plane. However, this stability is unacceptable in the regulation of flight because the plane vibrates a great distance. For a short period, it causes a defect in the fuselage at every transmission. This result dictates the use of a booster controller to reduce the impact of the conventional console that has different action points. An adaptive neuron controller was used to circumvent this problem. However, Figure (9) shows that the closed-loop system in the cross-section does not need a supported controller.

3. Neuron adaptive controller design

At this point, an adaptive controller is built using a neural network, and the neural network adds an enhanced control signal resulting from the correction PID (correction of the adaptive signal). The adaptive console compensates for the error caused by converting the non-linear model of a plane into a linear model. This result, in turn, allows the hew console (Adaptive+PID) by working on better, wider work points.

Figure (10) shows a box diagram of the proposed adaptive control system.

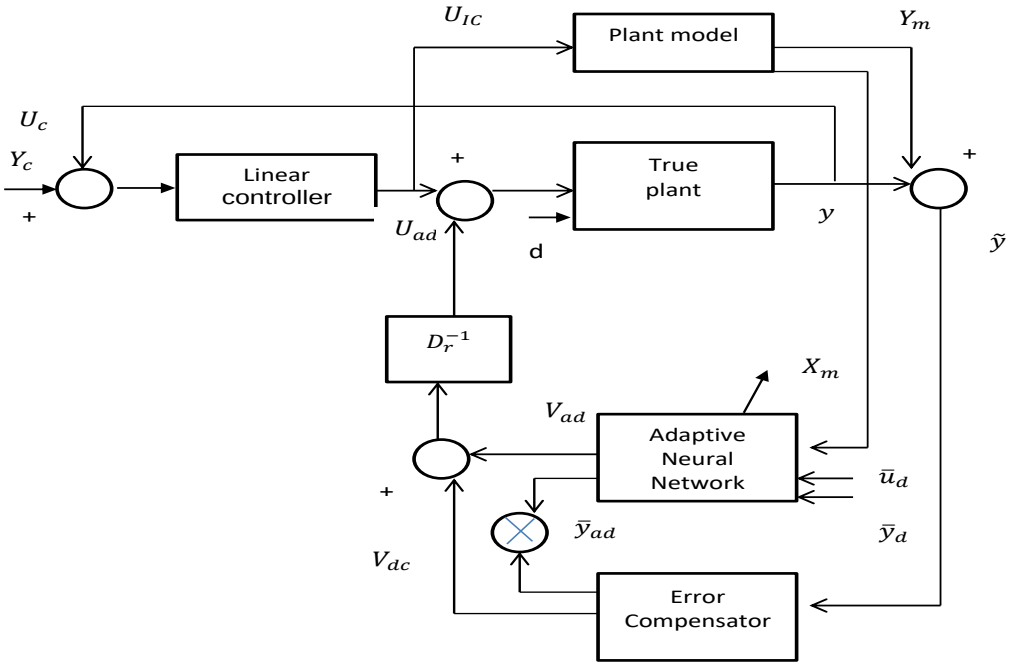

Figure (10) Proposed adaptive control system

In the upper ring, the linear controllers are designed to stabilise the near-linear model which is supposed to contain the main work of the real system. The term "main working mechanism" refers to a well-known and -defined work mechanism. In contrast, an unknown of the unmodified working mechanism is represented in the other loop, including the consequences of system transformation and triggers the linear controller is designed as we saw earlier. The idea here is to take advantage of the controller that was designed in the easiest possible way to consider the complexities that may be added. Therefore, the total closed-loop has the closest linear model, determining the best performance that can be obtained with adaptation. [10] The measured error between the top and bottom loops is simply the error between the outputs of near-linear model Y_m and real system Y. Thus, adaptive sign V_{ad} is added. In the conventional control, signal V_{Ic} compensates for the effect of the unmodified work and forces the lower ring to behave similarly as the upper ring. In other words, the idea involves feeding the conventional console with an adjustment component that allows the total console to drive system outlet y to chase retrograde output Y_m.

3.1 Adaptive addition to feedback

If adding an additional control signal (V_{ad}) to stabilise the error action and remove disturbances $\Delta(X, X_m, u)$, the signal due to the adaptive, the part can be expressed as:

$$V_{ad} = D_r^{-1}(V_{ac} - V_{ad}) \dots (1)$$

where (V_{dc}) is the result of the linear controllers, input $\tilde{y}$ is designed to stabilise the mechanism of error action when $\Delta(X, X_m, u) = 0$, and V_{ad} is the result of a neural network whose weights are modified in a way that allows estimating the response of the error.

The mechanism of error is expressed as follows.

$$\tilde{y}^{(r)} = -V_{dc} + V_{ad} - \Delta \ \dots (2)$$

The steps in [11] allow grading V_{ad} and V_{dc} based only on the available measurements.

Mouawad AL-Khatha has two different results .

$$[V_{dc}(s)\ \tilde{y}_{ad}(s)\ ] = \frac{1}{D_{dc}}[N_{dc}\ (s)\ N_{ad}\ (s)\ ]\tilde{y} \dots (3)$$

where the first result (V_{dc}) is designed to stabilise the mechanism of error, and the second result ($\tilde{y}_{ad}$) is an adaptive signal of a neural network that is equivalent to a linear merging of the error condition compensator and its input ($\tilde{y}$). By substituting the error (2), we obtain the following conversion function form.

$V_{ad} - \Delta \ to \ \tilde{y}_{ad}$:

$$\tilde{y}_{ad}(s)\frac{N_{ad}(s)}{S\ D_{dc}(s) + N_{dc}(s)}(V_{ad} - \Delta\ ) = G(s)(V_{ad} - \Delta\ ) \qquad \dots (4)$$

The non-linear neuron network is used to approximate disturbances (Δ). This approximation is fine if a set of displacement functions is selected over the approximation field. For example, [12] revealed that the continuous approximation of any degree of precision can be made using radial sequences.

To be $> o$, it can be approximated (Δ) using a linear neural network with limited weights (W) and a set of displacement functions ($\emptyset(.)$), such that

$$\Delta = W^T\emptyset(n), |\varepsilon(n)| < \varepsilon \dots (5)$$

where $\varepsilon(n)$ is the error in the approximation of the neural network, and n is the radiation of the entry network.

$$n(t) = [1\ X_m^T(t) u_d^T \underline{y}_d^T]$$

$$\underline{U}_d^T(t) = [u(t) \quad u(t-d) \dots \ u(t-(n_1 - r - 1)d)]^T$$

$$\underline{y}_d^T(t) = [y(t) \quad y(t-d) \dots \ y(t-n_1-1)d)]^T$$

$$\eta(t) = [1 X_m^T(t) u_d^T \underline{y}_d^T]$$

$$\underline{U_d^T}(t) = [u(t) \quad u(t-d) \dots u(t-(\eta_1 - r - 1)d)]^T$$

$$\underline{y_d^T}(t) = [y(t) \quad y(t-d) \dots y(t-(\eta_1 - 1)d)]^T$$

where $X_m^T(t)$ is the transmitted ray of the state variables of the system interventions. where $d > 0$ is a positive time delay, and r is the degree of the derivation of the system. The result of the adjustment part in Figure (1) is

$$\Delta = \widehat{w}^T \emptyset(\eta) \dots (6)$$

where $\widehat{w}$ is an estimate of weights w in Equation (s) which are adjusted in real time. To take measurements based on the measurements law,
G(s) must be positive. G(s) must be made positive by selecting $N_{ad}(s)$ correctly in case $r = 1$.
When $r > 1$, a low filter ($T^{-1}(s)$) must be added so that G(s) T(s) becomes positive.
Therefore,
$\tilde{y}_{ad}(s) = G(s)\, T(s)\, [T^{-1}(s)\, (V_{ad} - \Delta] \dots (7)$

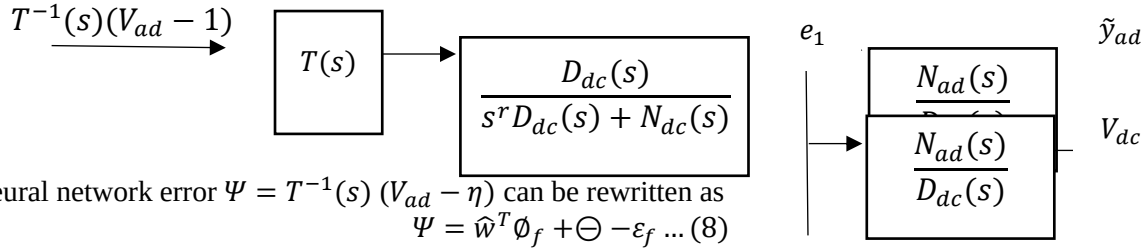

Neural network error $\Psi = T^{-1}(s)\, (V_{ad} - \eta)$ can be rewritten as

$$\Psi = \widehat{w}^T \emptyset_f + \ominus - \varepsilon_f \dots (8)$$

where ε_f and $\emptyset_f$ are the same ε and Φ after being nominated by candidate $T^{-1}(s)$, and $\ominus$ is the missing term and expressed as the following relationship:

$$\theta(s) = T^{-1}(s)(\widehat{w}^T \Phi) - \widehat{w}^T \emptyset_f \dots (9)$$

which can be terminated as follows:

$$\| \ominus \| \leq \propto \|\widetilde{w}\|_f \quad , \quad \propto > 0 \dots (10)$$

where $\widetilde{w} = \widehat{w} - w$ expresses the deviation of the estimated weights from the real weights. The conversation function from Ψ to e_1 is determined by the following equations:

$$Z_e = A_e Z_e + b_c \Psi \; e_1 = C_1^T Z_e \; \} \dots (11)$$

The conversion functions from $e_1 to\, \tilde{y}_{ad}$ and V_{dc} are defined as follows: $Z_{dc} = A_{dc} Z_{dc} +$
$b_{dr} e_1\, \tilde{y}_{ad} = C_{ad}^T Z_{dc} + d_{ad} e_1\, V_{dc} = C_{dc}^T Z_{dc} + d_{dc} e_1 \; \} \dots (12)$
where matrix A_{dc} is a stable matrix. By combining Equations (11) and (12), we obtain the equations described for the total error compensate shown in Figure (11).

$$Z = A_c Z + b_{c1} \Psi, ZaR$$

$$\tilde{y}_{ad} = C_{c1}^T\, Z\, V_{dc} = C_v^T\, Z\, e_1 = C_{e1}^T\, Z \; \} \dots (13)$$

where $A_{c1} = [A_c \; o \; b_{dc} C_1^T \; A_{dc}\,], b_{c1} = [b_c \; o\,], C_{c1}^T = \left[d_{ad} C_1^T \; C_{ad}^T\right]$
$C_v^T = \left[d_{dc}\; C_1^T \; C_{dc}^T\right], C_{e1}^T = [C_1^T \; o\,]$

Given that the transformation continues from Ψ to $\tilde{y}_{ad}$ from type strictly positive real (SPR), two matrices, $Q > 0$ and $p > 0$, exist so that the following Lyapunov's equation is achieved:

$$A_{c1}^T p + p A_{c1} + Q = 0$$

$$p b_{c1} = C_{c1}$$

Filter $T^1(s)$ is achieved as follows:

$$Z_f = A_f Z_f + b_f \emptyset, Z_f \in R^{n_f}$$

$$\emptyset_f = C_f^T Z_f$$

The filter from SPR is designed to be stable. Therefore, two matrices, $Q_f > 0$ and $P_f > 0$, exist so that the following Lyappunov's equation is achieved:

$$A_f^T p_f + p_f A_f + Q_f = 0$$

$\emptyset_r$ is used in the process of modifying the neural network weights as follows:

$$\widehat{w} = -\Gamma_w[\tilde{y}_{ad} Q_f + \sigma \widehat{w}]$$

where $\Gamma_w > o$ is the adjustment constant and determines the rate of the neural network's learning speed (σ). This constant expresses the rate of weight change of the adjustment parameter.

3.2 Results of the adaptive controller application

We used to construct the adaptive controller of a neural network from type RBF, where we installed the network weights between the elements of the input beam and the invisible layer. The number of elements of the hidden layers. The number of the elements of the output layer (1), and the number of elements of the input beam (12). The output layer element is linear. Filter $T^{-1}(s)$ has the following shapes:

$$T^{-1}(s) = \frac{1}{s+1}$$

Network weights speed coefficient $\Gamma_w = 20$.

Munificent unit 6 = 0.3. The mean, standard deviation of the diving function is $\sqrt{0.5}$. We used the line compensator described in the following figure, and the values were obtained through experiment.

$$[V_{dc}\ Y_{ad}\ ] = \frac{1}{s+45.6}[18(5+1.88)\ 255+20\ ]e_1$$

We selected this adaptive control model for plane model Aerosonde at the height of 200 m. It has a constant velocity of 30 M/S and a zero deviation angle. Thus, we obtained the following results. Figure (12) presents a comparison between the closed-loop responses of the diving angle to its square signal if the conventional controller is applied with and without neural network interference.

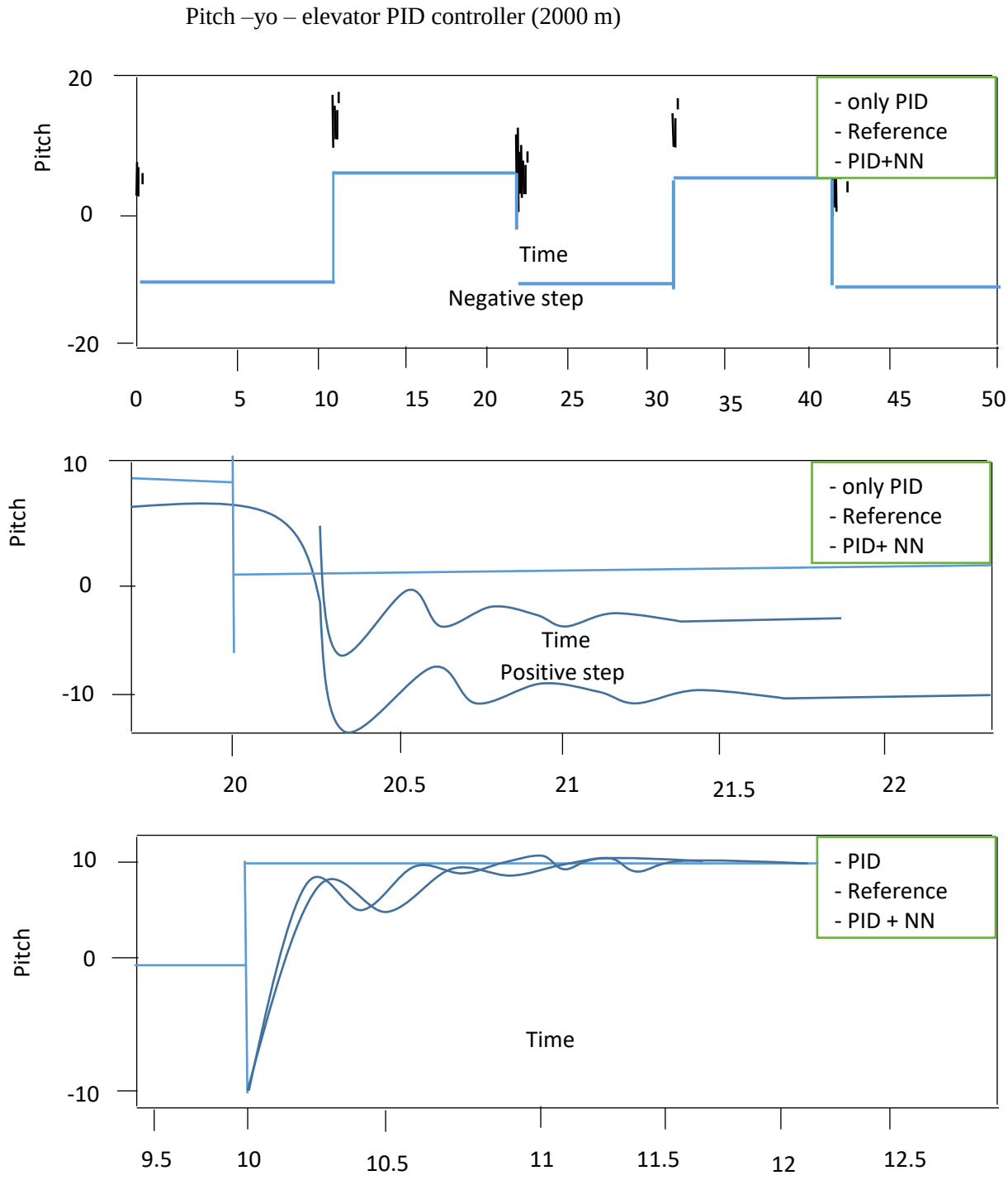

In figure (12), the closed-loop of the diving angle responded to the square indication in the case of a conventional controller and an adaptive controller 2000 m.

Figure (12) clearly shows that the neural network performed the error compensation process so that we obtained an acceptable.

Then, we tested this adaptive control model on plane model Aerosonde at a height 2000 m. It has a constant velocity of 30 m/s and a zero constant deviation angle. Thus, we obtained the following results. Figure (13) shows a comparison between the closed-loop responses of the diving angle to its square signal in the case of applying the conventional controller with and without the interference of a neural network.

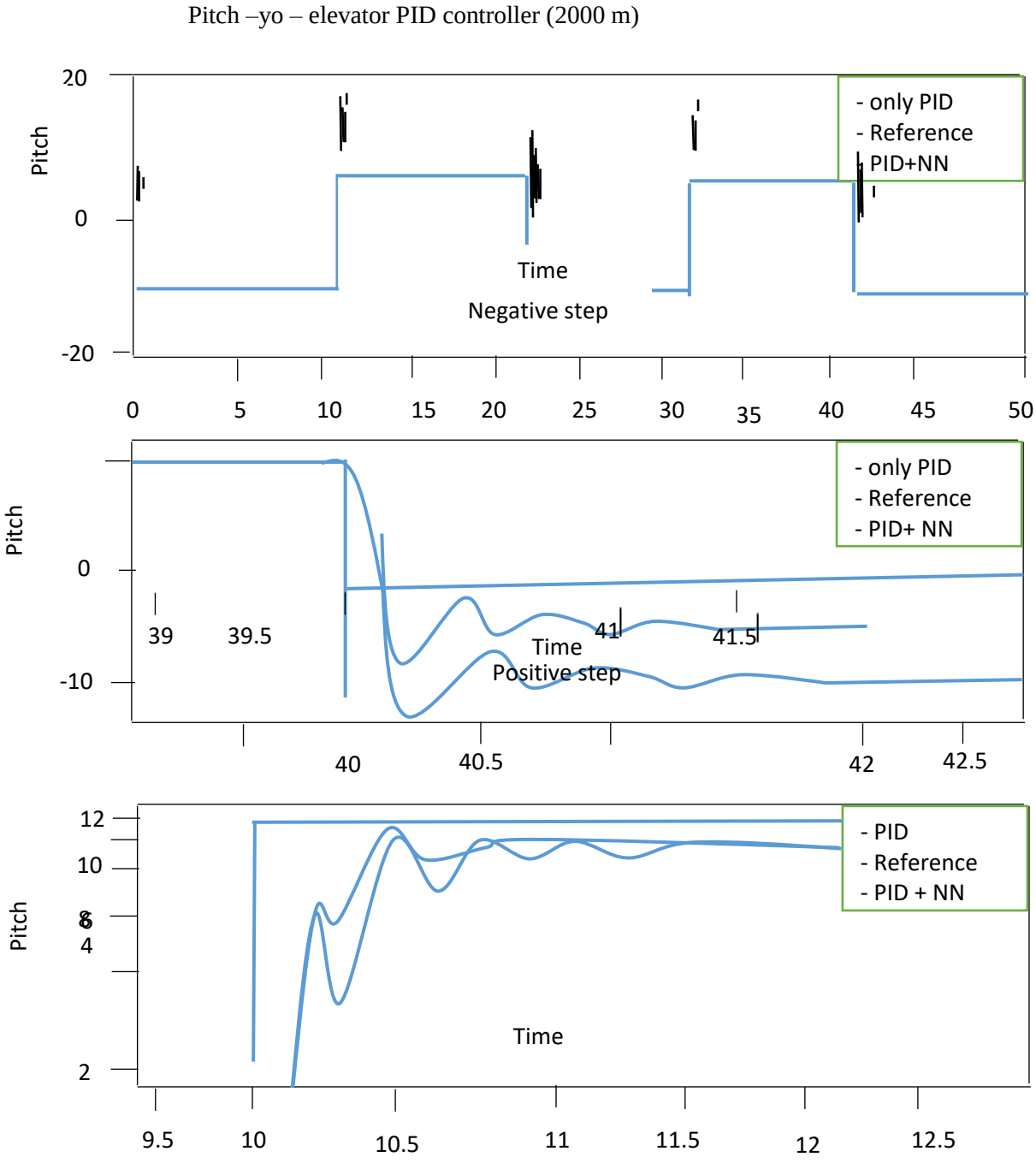

Figure (13) the closed-loop of the diving angle responds to the square signal in the case of a conventional controller

3-3 compare and test results

As we mentioned in the study of the source [4] on an adaptation algorithm that depends on a neural network that depends on real time. The network weights are adjusted according to the errors of system state variables by means of a specified cost dependent minimization according to Lapunov's second theory, by combining the neural network with a conventional controller, it was able to largely isolate the disturbances to which the entire plane was subjected.

Illustrated by the response displayed as shown in the figure (14).

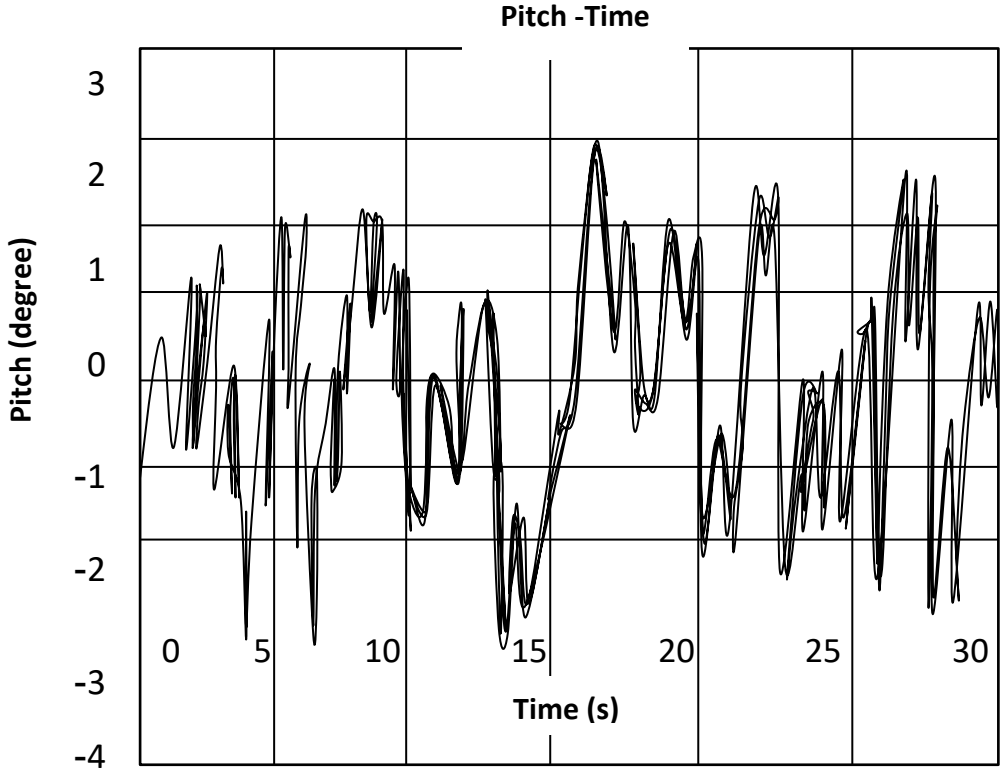

Figure (14) The difference between adaptive and conventional controller response

The neural network involved in the adaptation process plays a dampening role for the disturbances that the system is exposed to when it is controlled by the traditional controller alone.

Do not use the neural network in [4] to reduce the error rate 32% than in the case of the conventional controller alone, as mentioned.

Where as, the use of our neural network reduces the intensity of aliasing and vibration in the angle of the plane diving by a greater than 50% as shown in the figure [15].

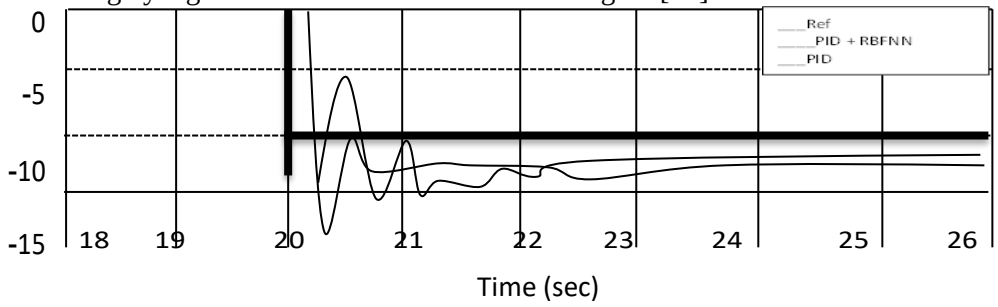

Figure (15) Closed loop response to diving angle

The neural network also contributed to mitigating the overrun to substandard 24% and thus it can be said that the use of adaptive controller in our research achieved better performance combine [7] between a floating system and a neural network to design a hybrid system that was used to control the changes of the diving angle of a drone plane and then moved to control altitude with the presence of this controller in the inner ring.
The response between them, as shown in the figure [16] showed the controller's ability to stabilize the elevation loop with slight overshoot and relatively large role vibrations. We in turn tested the elevation ring with the adoption of the angle of diving as an inner ring, and we obtained the result shown in the figure [17].

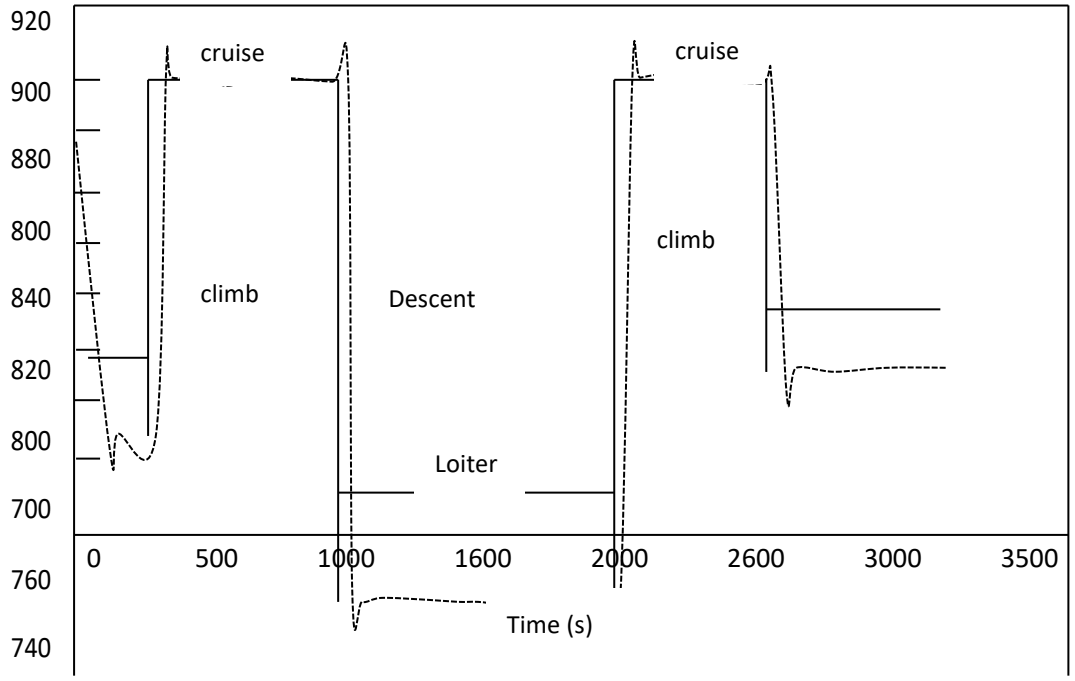

Figure (16)

We note that the response it has is better in terms of response time to a similar height difference 200m and from the override side, as well as from the standpoint a round the final position, thus it can be said that using the neural network in adapting to the added feed is better and easier than using the hybrid system.

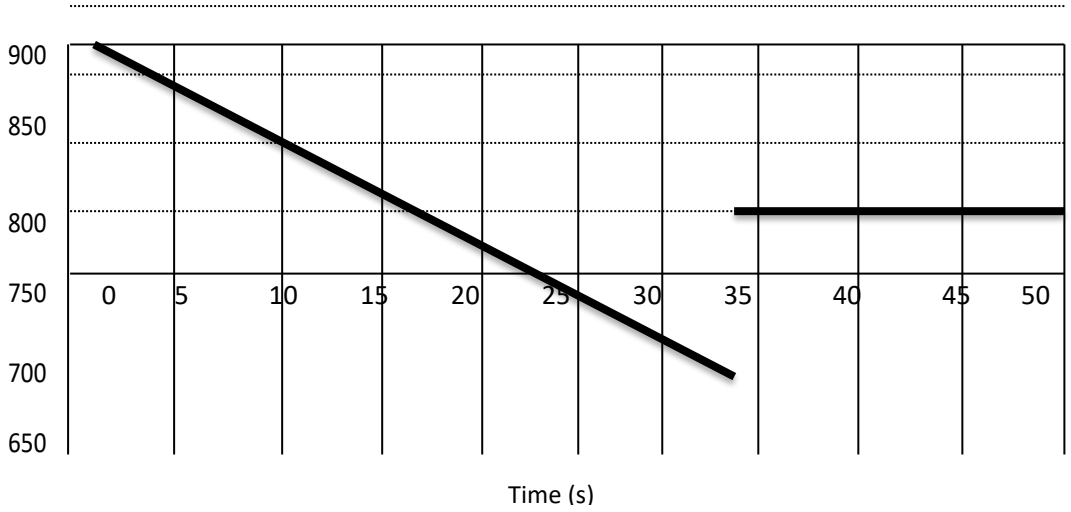

Figure (17)

The network can compensate for errors to obtain the desired response by exceeding 25% and a small static error.

In summary, the proposed adaptive controller can help achieve the optimal control of the model of the flying plane; in addition, it enables the expansion of the field of work of the plane. The proposed adaptive control system has the following advantages:

1- The basic control system structure is maintained.
2- The system works in real time
3- The system is technically simple to implement.
4- The system can be used to update existing systems or design new adaptive control systems.

References

[1] Anderson, John David, 2005 - **Introduction to flight**, volume 199. McGraw - Hill Boston 636p.
[2] Stevens, Brian Land Lewis, Frank L2003 - **Aircraft control and simulation**, John Wiley & Sons.
[3] Dydek, Zachary Thompson, 2010 - **Adaptive control of unmanned aerial systems**, PhD thesis, Massachusetts Institute of Technology, 129p.
[4] Lei, Xusheng and Ge, Shuzhi Sam and Fang, Jiancheng 2014 Adaptive Neural Network Control of Small Unmanned Aerial Rotorcraft, **Journal of Intelligent & Robotic Systems**, 75 (2): 331- 341.
[5] Boudjedir, Hana and Yacef, Fouad and Bouhali, Omar and Rizoug, Nassim, 2012 Adaptive Neural Network for a Quadrotor Unmanned Aerial Vehicle, **International Journal in Foundations of Computer Science and Technology**, 2: 1-13.
[6] Chowdhary, Girish and Johnson, Eric, 2007 Adaptive neural network flight control using both current and recorded data, **Guidance, Navigation and Control Conference**, AIAA-2007- 6505. Hilton Head.
[7] Farid, Ali Moltajaei, 2013 UAV Controller Based on Adaptive Neuro-Fuzzy Inference System and PID, **International Journal of Robotics and Automation** (IJRA). IAES 2(2):73-82.
[8] Chowdhary, Girish and Wu, Tongbin and Cutler, Mark and Ure, Nazim Kemal and How, Jonathan, 2012 Experimental Results of Concurrent Learning Adaptive Controllers, **Guidance, Navigation, and Control Conference**, Minneapolis In AIAA.
[9]Caughey, David A Sibley School of Mechanical & Aerospace Engineering, Cornell University, 201I Introduction to Aircraft Stability and Control,**Course Notes for M&AE 5070**, 14853-7501 pages, Ithaca, New York,
[10] Calise. J Anthony and Yang, Bong-Jun Hovakimyan, Naira 2002 An adaptive output feedback control methodology for non- minimum phase systems, **Conference on Decision and Control**, IEEE; .954--949 pages,1 volume
[11] Calise, Anthony J and Hovakimyan, Naira and Idan, Moshe.2001 Adaptive output feedback control of non-linear systems using neural networks, **Automatica**, 37(8):1201-1211.
[12] Robert M Sanner and Jean-Jacques E Slotine. 1992 Gaussian networks for direct adaptive control, **Neural Networks**, IEEE Transactions on, 3(6):837-863.
[13]- M. Pavella. P. G. Murthy. " Transient stability of Power System John Wiley & Sons Ltd. 1994.
[14]- Jeffery B. Burl, " Linear Optimal Control ", Addison- Wesley, Inc 1999."
[15] KAWTHER A. N. "NUMERICAL ANALYSIS & METHODS using MATLAB", IRAQ 2019.
[16] Wens, "Introduction to Ordinary and Partial Deferential Equations", spring, 2015.
[17] F.H.A.Rahim,N.N.Hawari and N.Z.Abidin,"Supply and demand of rice in Malaysia: system dynamics approach", International Journal of supply Chain and Management,Vol.6,No.4,pp.234-.240,2017
[18] Lars Skyttncr,General system Theory :Problems,perspectives,practice,second edition, world scientific publishing co,pte.LTD,2005.
[19] Falconer ,I.&Gottwald,G.A.&Melbourne ,I.(2007)"Application of the0-1 Test foe Chaos to Experimental Data"Xulvi-Brunet,SIAM.J,6,No.2.pp.395-402.
[20] KAWTHER ABBOOD NEAMAH,SAFA ABOOD.NAMA,Stabilization study of a non-linear self-regression model using linear approximation technique,2020
[21] Henning S .MortveitI,Christian M.Reidys (2008). An introduction to sequential Dynamical systems.springer ISBN0-387-30654-4

[22] B. Al Hayani and H. Ilhan, "Visual sensor intelligent module based image transmission in industrial manufacturing for monitoring and manipulation problems," *J. Intell. Manuf.,* **32,** 597–610 (2021).https://doi.org/10.1007/s10845-020-01590-1[22]
[23] B. Alhayani and H. Ilhan, "Hyper spectral image classification using dimensionality reduction techniques," *Int. J. Innov. Res. Electr. Electron. Instrum. Control Eng.*, vol. 5, no. 4, pp. 71–74, 2017.
[24] B. Al-Hayani and H. Ilhan, "Efficient cooperative image transmission in one-way multi-hop sensor network," *Int. J. Electr. Eng. Educ.*, vol. 57, no. 4, pp. 321–339, 2020.
[25] B. Al Hayani and H. Ilhan, "Image transmission over decode and forward based cooperative wireless multimedia sensor networks for Rayleigh fading channels in medical Internet of Things (MIoT) for remote health-care and health communication monitoring," *J. Med. Imaging Heal. Informatics*, vol. 10, no. 1, pp. 160–168, 2020
[26] B. Alhayani, H. J. Mohammed, I. Z. Chaloob, and J. S. Ahmed, "Effectiveness of artificial intelligence techniques against cyber security risks apply of IT industry," *Mater. Today Proc.*, 2021.
[27] B. Alhayani, S. T. Abbas, D. Z. Khutar, and H. J. Mohammed, "Best ways computation intelligent of face cyber attacks," *Mater. Today Proc.*, 2021
[28] Alhayani, B. and Abdallah, A.A. (2020), "Manufacturing intelligent Corvus corone module for a secured two way image transmission under WSN", Engineering Computations, Vol. ahead-of-print No. ahead-of-print. https://doi.org/10.1108/EC-02-2020-0107
[29] Alhayani, B., Abbas, S.T., Mohammed, H.J. *et al.* Intelligent Secured Two-Way Image Transmission Using Corvus Corone Module over WSN. *Wireless Pers Commun* (2021). https://doi.org/10.1007/s11277-021-08484-2